Original Article

JCBFM

Journal of Cerebral Blood Flow & Metabolism
2017, Vol. 37(8) 3001–3014

DOI: 10.1177/0271678X16680636
journals.sagepub.com/home/jcbfm
SAGE

Prevention of the collapse of pial collaterals by remote ischemic perconditioning during acute ischemic stroke

Junqiang Ma[1,2,3], Yonglie Ma[2], Bin Dong[2], Mischa V Bandet[1,2], Ashfaq Shuaib[1,4] and Ian R Winship[1,2]

Abstract

Collateral circulation is a key variable determining prognosis and response to recanalization therapy during acute ischemic stroke. Remote ischemic perconditioning (RIPerC) involves inducing peripheral ischemia (typically in the limbs) during stroke and may reduce perfusion deficits and brain damage due to cerebral ischemia. In this study, we directly investigated pial collateral flow augmentation due to RIPerC during distal middle cerebral artery occlusion (MCAo) in rats. Blood flow through pial collaterals between the anterior cerebral artery (ACA) and the MCA was assessed in male Sprague Dawley rats using in vivo laser speckle contrast imaging (LSCI) and two photon laser scanning microscopy (TPLSM) during distal MCAo. LSCI and TPLSM revealed that RIPerC augmented collateral flow into distal MCA segments. Notably, while control rats exhibited an initial dilation followed by a progressive narrowing of pial arterioles 60 to 150-min post-MCAo (constricting to 80–90% of post-MCAo peak diameter), this constriction was prevented or reversed by RIPerC (such that vessel diameters increased to 105–110% of post-MCAo, pre-RIPerC diameter). RIPerC significantly reduced early ischemic damage measured 6 h after stroke onset. Thus, prevention of collateral collapse via RIPerC is neuroprotective and may facilitate other protective or recanalization therapies by improving blood flow in penumbral tissue.

Keywords

Collateral circulation, ischemia, laser speckle contrast imaging, neuroprotection, two-photon microscopy

Received 7 July 2016; Revised 23 September 2016; Accepted 30 October 2016

Introduction

Flow through cerebral collaterals is increasingly recognized as a key variable in determining outcome after acute ischemic stroke. The cerebral collaterals are auxiliary vascular pathways that can partially maintain blood flow to ischemic tissue when primary vascular routes are blocked.[1–4] The circulatory anastomoses that constitute the Circle of Willis are classified as "primary" collaterals,[5] while the "secondary" collaterals include the pial or leptomeningeal collaterals.[6] Pial collaterals are anastomotic connections located on the cortical surface which connect distal branches of the anterior, middle, and posterior cerebral arteries (ACA, MCA, and PCA). Blood flow through pial collaterals after occlusion of the principal supplying artery (e.g. the MCA) allows retrograde filling of vessels in the ischemic penumbra. Good collateral flow is associated with reduced infarct core, improved prognosis, and better response to recanalization therapy.[7–10] Therapies that can augment collateral flow may

[1]Neuroscience and Mental Health Institute, University of Alberta, Edmonton, AB, Canada
[2]Neurochemical Research Unit, Department of Psychiatry, University of Alberta, Edmonton, AB, Canada
[3]The First Affiliated Hospital, Shantou University Medical College, Shantou, China
[4]Department of Medicine, Division of Neurology, University of Alberta, Edmonton, AB, Canada

Corresponding author:
Ian R Winship, 12-127 Clinical Sciences Building, Edmonton, AB T6G 2R3, Canada.
Email: iwinship@ualberta.ca

therefore protect penumbral tissue and augment recanalization.[11]

Ischemic conditioning was introduced in the 1980s[12] as a treatment to induce a tissues' endogenous protection against ischemic injury by the application of repetitive, brief ischemic periods before or after more severe ischemic insults (referred to as local pre- and post-conditioning, respectively). A significant breakthrough in the study of ischemic conditioning as a protective therapy was the discovery that ischemic conditioning induced at an organ remote to the site of severe ischemia (termed "remote ischemic conditioning"), such as the limb in the case of cerebral ischemia, can also protect target tissue.[13] Crucially, remote ischemic conditioning can be applied prior to stroke (termed remote ischemic preconditioning), after the onset of ischemia (termed remote ischemic per-conditioning (RIPerC), or at the time of reperfusion (termed remote ischemic post-conditioning) (Figure 1(a)).[14] RIPerC has promise as an acute ischemic stroke treatment that can be applied during the ischemic period whether patients receive reperfusion treatment (e.g. rt-PA) or not.[13] Preliminary preclinical and clinical data suggest that RIPerC may be neuroprotective.[15–23] However, relatively little is known about the underlying protective mechanisms of RIPerC. Recent data suggest that RIPerC may increase cerebral blood flow,[18,24] but its ability to augment collateral circulation has not been assessed. The objective of this study was to use advanced in vivo imaging to define changes in pial collateral flow during RIPerC. Here, high resolution in vivo laser speckle contrast imaging (LSCI) and two photon laser scanning microscopy (TPLSM) were used to map dynamic changes in pial collaterals during RIPerC after distal middle cerebral artery occlusion (MCAo) in rats. Our findings demonstrate that RIPerC induced by bilateral femoral artery occlusion (BFO) augments blood flow through pial collaterals by preventing their collapse or constriction over time.

Methods

Male Sprague–Dawley rats (2–5 months of age, $n = 47$) were used. Prior to experimental procedures, animals were housed in pairs on a 12-h day/night cycle and had access to food and water ad libitum. Procedures conformed to guidelines established by the Canadian Council on Animal Care, were approved by the Health Sciences Animal Care and Use Committee at the University of Alberta, and are reported in a manner consistent with the ARRIVE (Animal Research: Reporting in Vivo Experiments) guidelines. The experimental timeline is illustrated in Figure 1(b). Sample sizes estimates were based on variability in data from previous LSCI and TPLSM experiments in our laboratory.

Anesthesia and monitoring

For LSCI experiments, anesthesia was induced with 4–5% isoflurane and maintained at ~1.0–1.5% isoflurane (in 70% nitrous oxide and 30% oxygen). Rats ($n = 11$ for each of the RIPerC and control groups) remained under isoflurane until completion of the imaging experiments, at which point they were removed from anesthetic until euthanasia 6 h after MCAo onset. While isoflurane allows stable and reliable anesthesia, it is a volatile inhalant anesthetic, has been associated with vasodilation or impaired vasoreactivity, and may mask neuroprotection during cerebral ischemia.[25–29] Nonetheless, published studies of collateral therapeutics from our group and others suggest that augmented collateral flow and/or neuroprotection is apparent with isoflurane anesthesia as well as alternative anesthetics (e.g. urethane or sodium pentobarbital).[1,30–32] Nonetheless, our quantitative analyses of pial arteriole diameter using TPLSM were performed under urethane anesthesia to allow a comparison of vascular effects and degree of neuroprotection observed under isoflurane against a different anesthetic paradigm. While wakefulness and depth of anesthesia alter hemodynamics, the mechanisms of action for urethane spare many pathways involved in neurovascular coupling and recent studies support its use in studies of cerebral hemodynamics.[33–36] Therefore, for TPLSM experiments, rats ($n = 8$ for each of the RIPerC and control groups) were anaesthetized with urethane (i.p. 1.25 g/kg, divided into four doses delivered at 30-min intervals), then remained anaesthetized until euthanasia. During all surgery and imaging, temperature was maintained at 36.5–37.5°C with a thermostatically controlled warming pad and heart rate, oxygen saturation, and breath rate were monitored using a pulse oximeter (MouseOx, STARR Life Sciences). In a separate cohort of isoflurane anesthetized rats ($n = 6$ RIPerC and 3 controls rats), blood pressure monitoring was performed via catheter in the ventral tail artery after MCAo and throughout RIPerC or sham treatment using a PressureMAT monitor (PendoTECH).

Cranial windows

LSCI and TPLSM were performed through cranial windows using a thin skull preparation or a craniotomy, respectively.[37,38] For thin skull imaging, a midline incision was made on the scalp to expose the surface of the skull (Figure 1(d)). A ~6 × 4-mm section of the skull over the distal regions of the right MCA territory was thinned until translucent using a dental drill (frequently flushing with saline to dissipate heat). The outer skull layer and subjacent spongy bone were cleaned and smoothed by round scalpel, allowing

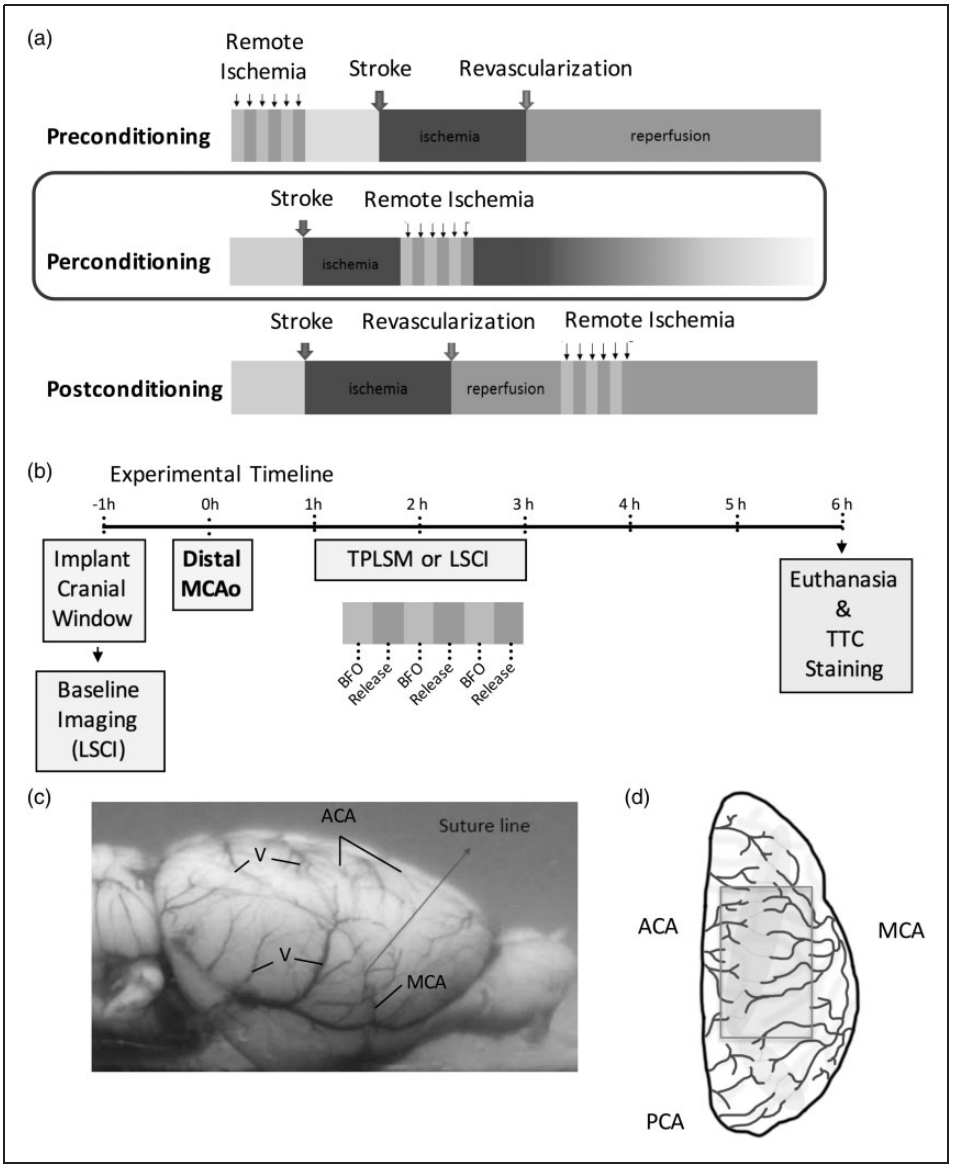

Figure 1. (a) Remote ischemic conditioning can be applied prior to stroke, after the onset of ischemia, or at the time of reperfusion (termed remote ischemic pre-, per-, or post-conditioning, respectively) (b) Experiment timeline. (c) A lateral view of the rat brain showing the location of ligation of the right middle cerebral artery (MCA) above the rhinal fissure that was used to induce distal occlusion of the MCA (MCAo). (d) A schematic of the dorsal surface of the rat cortex illustrating the placement of cranial imaging window over the distal territories of anterior cerebral artery (ACA) and MCA (modified with permission from Winship et al.[1]). TPLSM: two photon laser scanning microscopy; LSCI: laser speckle contrast imaging; TTC: 2,3,5-triphenyltetrazolium chloride staining; V: surface vein.

surface vessels to be visualized through the remaining thin layer of bone. A layer of mineral oil was applied to the window and sealed with a cover slip. Procedures for cranial windows via craniotomy were identical, except the skull over the right MCA territory was thinned until translucent using a dental drill and then gently removed. The cranial window was covered with a thin layer of 1.3% low-melt agarose, and sealed with a coverslip.[1,38]

RIPerC via BFO

Femoral arteries were dissected from accompanying veins and nerves below the groin ligaments. RIPerC was initiated 60-min post-MCAo by occluding and releasing the femoral arteries bilaterally with vascular clamps for 3 cycles (each 15 min ON/OFF). Control rats received a sham surgery with equivalent anesthesia and arterial isolation but did not receive BFO.

LSCI

LSCI measures real time changes in cerebral blood flow with high spatial and temporal resolution in a two-dimensional, wide field of view.[39–41] By recording laser speckle on the surface of the cerebral cortex using a CCD camera with fixed exposure time, speckle blurring can be quantified to determine speckle contrast K. To collect LSCI data, rats were secured in ear bars on a custom-built stereotaxic plate under a video macroscope with a tandem lens configuration ($\times 1.7$ magnification) and a Dalsa 1M60 Pantera camera.[1,37,38] A Thorlabs LDM 785S laser (20 mW, wavelength of 785 nm) was used to illuminate the rat cortex at about 30° incidence. Stacks of 100 sequential images (1024×1024 pixels) were acquired at 20 Hz (5 ms exposure time) during each imaging session. LSCI was performed before MCAo, 60-min post-MCAo (before RIPerC or sham treatment), and continued during 90 min of RIPerC (or sham) at 15-min intervals. All processing and analysis of laser speckle images were performed using ImageJ software (NIH) by a blinded experimenter. Maps of speckle contrast were made from the collected images of raw speckling by determining the speckle contrast factor K for each pixel in an image. K is calculated as the ratio of the standard deviation to the mean intensity ($K = \sigma_s/I$) in a small (5×5 pixels) region of the speckle image.[39–41] K ranges from 0 to 1. When the scattering particles (blood cells) are moving very fast, the speckle K will be very close to 0. Plots of K therefore show maps of blood flow with darker vessels illustrating faster blood flow velocity. To measure blood flow velocity within identified arteriole segments within or downstream of anastomoses (referred to as MCA segments or pial arterioles in the results section), speckle contrast profiles (Figure 3(a)) along multiple cross-sections of the anastomoses joining the distal ACA and MCA segments as well as segments of the MCA downstream of ACA anastomoses were extracted. The value of K at the center of these profiles (i.e. the speckle contrast K at the minima of the profile, Figure 3(a)) represents the vessel midline blood flow velocity. A better estimate of relative changes in blood flow velocity through these collateral channels was then attained by converting these centerline K values to correlation times (τ_c) using the equation

$$K^2 = \frac{\tau_c}{2T}\left\{1 - \exp\left(\frac{-2T}{\tau_c}\right)\right\}$$

where T is the exposure time of the camera. τ_c values are approximately inversely proportional to the speed of the blood flow (i.e. $1/\tau_c$ is considered proportional to the blood flow velocity).[1,42] Because anastomoses were generally not well-resolved prior to MCAo, analysis was performed on changes in vessel flow relative to post-MCAo measures (i.e. measurements recorded 60 min after MCAo onset). Blood flow velocity changes relative to 60-min post-MCAo (pre-treatment) are therefore illustrated as $\tau_{\mathrm{PostMCAo}}/\tau_c$.

Diameter was determined for ACA-MCA anastamoses and MCA segments downstream of using an ImageJ plug-in that uses a full-width at half-maximum algorithm to estimate the inner vessel diameter using the same vessel profiles used to determine velocity (Figure 3(a)).[1,4,32,43] Vessel conformation and orientation can change between baseline imaging and post-MCAo image collection due to subtle difference in placement in the head holder and due to swelling and edema that may shift brain tissue under the cranial window following induction of MCAo. Moreover, anastomotic sections are typically not visible prior to ischemic onset, as the diameter and/or velocity of flow may be below resolution for LSCI. For these reasons, intravessel velocity and diameter measurements are presented as relative changes (percent change) from values measured 60 min after induction of MCAo (i.e. post-MCAo but pre-treatment). After this time point, vascular anatomy remains consistent in LSCI data and repeated measurements are not an issue.

To estimate changes in blood flow using a measure that incorporates changes in vessel midline blood flow velocity and diameter, relQ[1] was calculated using the formula

$$\mathrm{relQ} = \pi r_n^2(\tau_{\mathrm{PostMCAo}}/\tau_c)$$

where r_n is the mean radius of the MCA segments in a given animal normalized to the radius at 60-min post-MCAo for that animal (i.e. Post-MCAo (pre-treatment) $r_n = 1$ and $\tau_{\mathrm{PostMCAo}}/\ \tau_c = 1$, such that Post-MCAo $\mathrm{relQ} = \pi$).

TPLSM

After implantation of the cranial window, fluorescein isothiocyanate–dextran (70,000 MW, Sigma-Aldrich) was injected via the lateral tail vein (0.3 ml, 5% (w/v) in saline). In vivo microscopy was then performed using a Leica SP5 MP TPLSM and Coherent Chameleon Vision II pulse laser tuned to 800 nm. Z-stacks through the first 200 μm of cortical tissue were acquired through the cranial window using a $10 \times$ water dipping objective (Leica HCX APO L10×/0.3 W) and vessel diameter measurements were made from maximum intensity projections of these stacks using the same ImageJ plug-in (full-width at half-maximum algorithm) used in LSCI experiments.[43] While the repeated imaging schedule (15-min intervals) did not allow a comprehensive analysis of blood flow velocity with these regions of

interest, red blood cell (RBC) velocity was measured in three to five vessels per region. For analysis of blood flow velocity, line scans were conducted on identifiable arterioles (>10-μm diameter). Blood flow velocity measurements were determined from line scan images by calculating the inverse slope of the linear streaks made by RBCs.[44,45]

Distal MCAo

Cerebral ischemia was induced by distal MCA ligation (Figure 1(c)) in conjunction with bilateral common carotid artery (CCA) ligation.[46] This model is relevant to the most common type, location, and outcome of human stroke (distal MCAo with cortical infarct). By blocking the proximal cortical branch of MCA, this model generates well-defined ischemia in the MCA cortical territory and allows for a consistent blood flow reduction and infarct with rapidly developing neurological impairment. Distal MCA ligation and imaging protocols were performed by different individuals, and surgeons inducing ischemia were blind to the experimental group for each rat. CCAs were accessed through ventral midline cervical incisions and ligated with 4–0 prolene sutures below the carotid bifurcation. A temporal incision was then made and the right temporalis muscle was gently separated from the bone. A burr hole of 1.5 mm in diameter was made through the squamosal bone, the dura was removed, and the cortical MCA was visualized. The exposed distal MCA was isolated and ligated with a square knot by atraumatic 9–0 prolene suture above the rhinal fissure (Figure 1(c)).

Triphenyl tetrazolium chloride staining

All rats were euthanized 6 h after induction of the MCAo. The brains were rapidly removed and sliced into seven coronal, 2 mm sections using a brain matrix, then incubated in 2% 2,3,5-triphenyltetrazolium chloride (TTC) solution at 37°C for assessment of mitochondrial dehydrogenase activity. Tissue damage was assessed in digital images of TTC-stained tissue by a blinded experimenter using ImageJ (NIH) software. Volume of tissues showing early ischemic damage is expressed as a percentage of hemisphere. These measures were calculated for each tissue slice using the indirect method[47,48] to control for tissue distortion due to edema using the following equation

$$\text{Volume of ischemic damage (\% hemisphere)} = \left[\sum(A_C - A_{NI}) / \sum(A_C)\right] \times 100$$

where A_C is the area of the hemisphere contralateral to stroke in a given tissue slice and A_{NI} is the area of the non-injured tissue (i.e. non-ischemic tissue that stains red using TTC) in the ipsilateral (stroke affected) hemisphere of the same slice.

Statistics

Graphpad Prism was used for all statistical analyses. Two-way repeated measures ANOVAs were used to compare effects of RIPerC or sham treatment on vessel diameter, blood flow velocity, and *RelQ*. Post hoc comparisons were performed using Sidak's multiple comparisons test. Volumes of ischemic tissue damage (% hemisphere) were compared using an unpaired Student's *t*-test. Linear regression analyses were performed to determine to what extent the proportion of variance in the volume of tissue damage could be accounted for by variance in measures of MCA (pial arteriole) diameter or blood flow velocity in ischemic regions.

Results

LSCI of collateral blood flow

LSCI produced high-resolution images of collateral flow from the ACA into the distal segments of the MCA (Figure 2(a)). LSCI maps of blood flow were acquired prior to MCAo, 60 min after MCAo but prior to RIPerC (or sham surgery), and during each 15-min cycle of BFO or release (3 cycles, Figure 1(b)). Figure 2(a) and (b) illustrates representative LSCI data from RIPerC and control rats, respectively. Panels (from left to right) show surface flow before MCAo, 60 min after distal MCAo, during the 3rd cycle of BFO or sham treatment (60–75-min post-stroke), and during the 3rd cycle of release or sham treatment (75–90-min post-stroke), respectively. In both groups, anastomoses join the distal segments of the ACA and MCA after MCAo. Neither RIPerC rats or controls exhibited dramatically altered patterns of pial collateral blood flow following treatment. However, a reduction in speckle contrast (increased flow) in LSCI maps from RIPerC-treated rats contrasts with an apparent increase in speckle contrast over time in controls. Notably, this apparent increase in blood flow could not be explained by central hemodynamic effects, as there was no significant main effect of treatment or a significant treatment × time interaction ($P > .05$) on arterial blood pressure (Figure 2(b)), oxygen saturation (Figure 2(c)), heart rate (Figure 2(d)), or breath rate (Figure 2(e)).

Changes in pial arteriole diameter and blood flow

Changes in diameter, blood flow velocity, and an overall flow (*RelQ*) during RIPerC or sham treatment were determined for distal branches of the MCA adjacent or

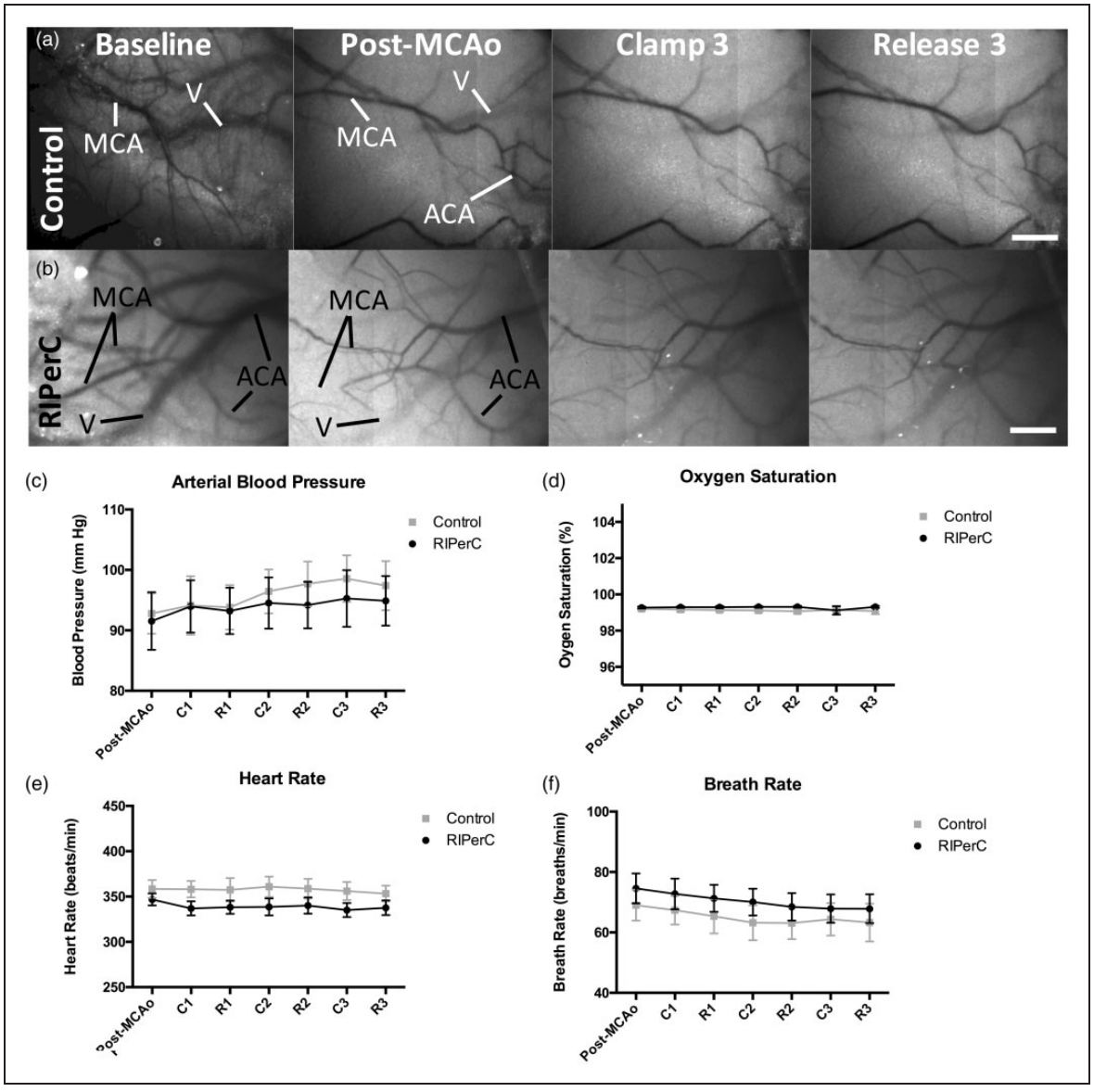

Figure 2. (a, b) Representative LSCI maps of collateral flow in a RIPerC treated and control rat. Panels (from left to right) show surface flow before middle cerebral artery occlusion (MCAo), 60 min after distal MCAo, during the third cycle of bilateral femoral occlusion (BFO) or sham treatment (60–75-min post-stroke), and during the third cycle of release or sham (75–90-min post-stroke), respectively. Overall, darkening of LSCI maps (from post-MCAo until final imaging) in RIPerC-treated animals suggests RIPerC is associated with an increase in flow in the imaging window. Scale bar, 1 mm. (c–f) RIPerC was not associated with central hemodynamic effects as arterial blood pressure ($n = 6$ RIPerC rats and 3 controls), oxygen saturation ($n = 10$ RIPerC and 8 controls), heart rate ($n = 10$ RIPerC and 8 controls), and breath rate ($n = 10$ RIPerC and 8 controls) were unchanged by treatment relative to controls. Graphs show mean ± s.e.m. MCA: middle cerebral artery; ACA: anterior cerebral artery; V: surface vein; C1: 1st cycle of clamp; R1: 1st cycle of release; C2: 2nd cycle of clamp; R2: 2nd cycle of release; C3: 3rd cycle of clamp; R3: 3rd cycle of release.

downstream of collateral anastomoses with the ACA (Figure 3(a)). Mean LSCI data ($n = 11$ per treatment group) are shown in Figure 3(b) to (d). Diameter of ACA-MCA anastomoses and downstream MCA segments (mean ± s.e.m., 83.4 ± 4.7 μm) (Figure 3(b)) exhibited a significant main effect of treatment group ($F_{(1,\ 20)} = 17.75$, $P = 0.0004$). Sidak's post hoc comparisons revealed that RIPerC-treated rats had significantly larger MCA segment diameters at all-time points (C1 = 1st cycle of clamp, R1 = 1st cycle of release…) during treatment relative to controls (left panel). Notably, MCA segments dilate following MCAo, so these differences reflect further dilation in RIPerC-treated animals contrasted with a gradual

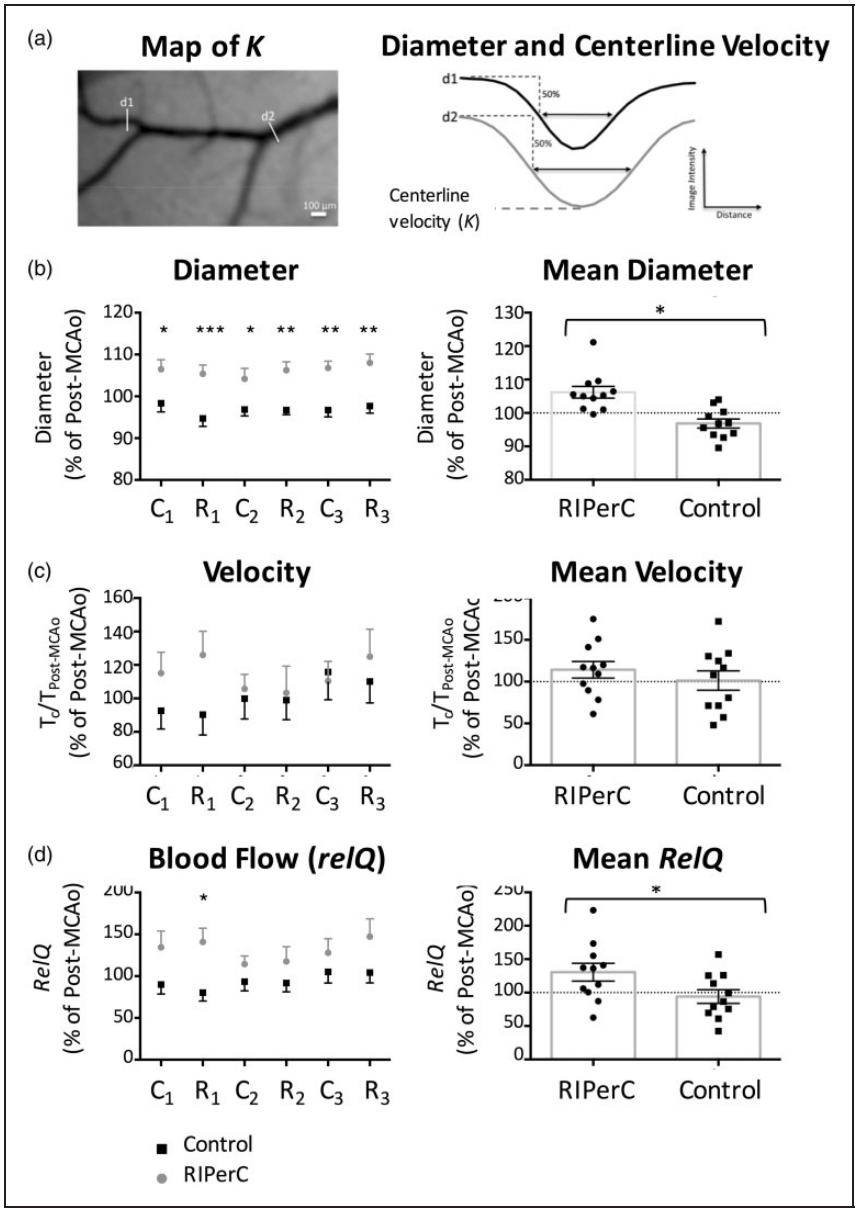

Figure 3. (a) Diameter and centerline blood flow velocity measures could be derived from profiles of speckle contrast spanning middle cerebral artery (MCA) segments. LSCI was used to determine relative changes in diameter (b) and blood flow velocity (c) in anterior cerebral artery (ACA)-MCA anastomoses and distal MCA segments. (b) RIPerC-treated rats ($n = 11$) had significantly larger diameters at all-time points during treatment relative to controls ($n = 11$) (left panel, mean changes in diameter during the complete treatment period are illustrated at right). (C) Shows mean changes in correlation times (τc) relative to post-MCAo values. No significant main effect of treatment was observed. (d) Overall flow in these pial arterioles was estimated by calculating *RelQ*. A significant main effect of treatment on *RelQ* was observed, suggesting the greatest difference in flow during the 1st cycle of BFO release. *$P < 0.05$; **$P < 0.01$; ***$P < 0.001$. Graphs show mean ± s.e.m. MCAo: middle cerebral artery occlusion; C1: 1st cycle of clamp; R1: 1st cycle of release; C2: 2nd cycle of clamp; R2: 2nd cycle of release; C3: 3rd cycle of clamp; R3: 3rd cycle of release.

narrowing of these vessels in controls. Notably, single sample *t*-tests shows that the dilation due to RIPerC and the narrowing in control rats represents significant changes relative to post-MCAo values ($P = .006$ and .040, respectively, against a hypothetical post-MCAo of 100%). Figure 3(c) shows mean changes in blood flow velocity (correlation times, τ_c) relative to post-MCAo. No significant main effect or interaction was observed ($P > .05$). Overall, flow in MCA segments was estimated by calculating *RelQ* (Figure 3(d)). A significant main effect of treatment on *RelQ* was observed ($F_{(1,\ 20)} = 4.686$, $P = 0.0427$), with Sidak's comparisons suggesting the greatest difference in flow during the 1st cycle of BFO release.

Diameter measurement using TPLSM

LSCI data suggest increased flow through collateral vessels after MCAo primarily due to a difference in the diameter of MCA segments between treatment groups. While LSCI measurements of diameter have been previously validated,[1] they are an indirect measure of luminal diameter based on the speckle contrast. Additionally, LSCI experiments were performed under isoflurane anesthesia, which may itself induce vasodilation and partially mask treatment effects. TPLSM was therefore performed to directly assess the luminal diameter of anastomoses and pial MCA segments during RIPerC or sham treatment after distal MCAo in urethane anaesthetized rats (Figure 4, $n = 8$ per treatment group). Moreover, TPLSM allowed measurement of luminal diameter in smaller pial collaterals (mean $\pm$ s.e.m., $40.2 \pm 3.1\,\mu m$) that could not always be reliably measured with wide field LSCI. Figure 4(b) shows maximum intensity projections of pial vessels from the region demarcated (white box) in the cranial window shown in Figure 4(a) from a control rat. Pial vessels were imaged 60 min after MCAo and again at 15-min intervals during the following 90 min (Figure 4(b)). Narrowing of MCA segments over time after MCAo was apparent in controls (Figure 4(b) and (d)) but did not occur in RIPerC-treated animals (Figure 4(f) and (h)). A significant main effect of treatment group on MCA segment diameter and a significant interaction between treatment and time was observed (Figure 4(c); *Treatment,* $F_{(1,\ 14)} = 12.$, $P = 0.0031$; *Time,* $F_{(5,\ 70)} = 12.$, $P = 0.0031$; *Interaction,* $F_{(5,\ 70)} = 6.586$, $P < .0001$). Sidak's post hoc comparisons revealed that RIPerC-treated rats had significantly larger diameters at all-time points after the initial BFO clamp. Mean diameters (in μm) for MCA segments in RIPerC and control rats are shown in Figure 4(e) and (g), respectively. In the RIPerC groups, diameters did not change significantly over time (Repeated measures ANOVA, $P > .05$). However, a significant main effect of time was observed in the control rats ($F_{(6,\ 42)} = 9.347$, $P < 0.0001$) and Sidak post hoc comparisons confirmed significantly smaller diameters relative to baseline during imaging at R1, C2, R2, C3, and R3 (all $P < .001$). No main effect of treatment or significant interaction between time and treatment was detected for measures of RBC velocity in vessels within these regions ($P > .05$).

Early ischemic damage

TTC staining revealed a significant reduction in the volume of tissue showing early ischemic damage in rats treated with RIPerC (Figure 5, right panel, Student's *t*-test, $P = .0001$). Regression analyses were performed to examine volume of tissue damage as a function of LSCI- and TPLSM-derived measures of pial arteriole diameter and blood flow velocity (Figure 6). To examine if narrowing of MCA segments over time after MCAo was associated with increased ischemic damage, a regression analysis of the volume of early ischemic damage (from TTC-stained tissue) as a function of arteriole diameter at the final imaging time point was performed. Figure 6(a) shows a plot of damage (% of hemisphere) as a function of vessel diameter for all rats from both LSCI and TPLSM studies ($n = 38$, collapsing 19 rats each from RIPerC and control groups onto a single plot). A significant linear relationship between damaged tissue volume and vessel diameter was observed ($R^2 = 0.13$, $P = .024$), with increased narrowing from post-MCAo values being associated with greater infarct volume. The statistical relationship was strengthened when regression analyses were confined to more quantitative measurements of MCA segments from TPLSM experiments (Figure 6(b), $R^2 = 0.36$, $P = .014$).

To examine if tissue damage was associated with changes in regional blood flow velocity relative to baseline (pre-MCAo) values, a second regression analysis was performed. For this regression analysis, relative flow changes from baseline (pre-MCAo) were measured in a contiguous ROI consisting of a 500×500 pixel square positioned to include the distal MCA and ACA segments. Such regional measures of speckle contrast correlate highly with other measures of regional cerebral blood flow such as laser Doppler flowmetry,[49] and allowed inclusion of pre-MCAo baseline values (whereas diameter and velocity measurements can be difficult to attain from anastomoses that are not well-resolved prior to ischemia). Mean correlations times normalized to baseline (pre-MCAo, $\tau_{Baseline}/\tau_c$) values are illustrated for the post-MCAo (pre-treatment) time point in Figure 6(c). Additionally, the mean $\tau_{Baseline}/\tau_c$ measured during the treatment period is illustrated (i.e. this mean $\tau_{Baseline}/\tau_c$ was calculated by determining the average of the six values measured during the 3 cycles of clamp and release). Consistent with intravessel measures from MCA segments (Figure 3(c)), multivariate analysis did not reveal a significant main effect of treatment or a significant time $\times$ treatment interaction on $\tau_{Baseline}/\tau_c$ calculated from the regional ROI. In Figure 6(d), volume of tissue showing signs of early ischemic damage is plotted as a function of regional flow velocity ($\tau_{Baseline}/\tau_c$) for all animals in LSCI and TPLSM studies. A significant linear relationship between damaged tissue volume and regional blood flow was observed ($R^2 = 0.30$, $P = .008$) with higher $\tau_{Baseline}/\tau_c$ values being associated with smaller volumes of tissue damage.

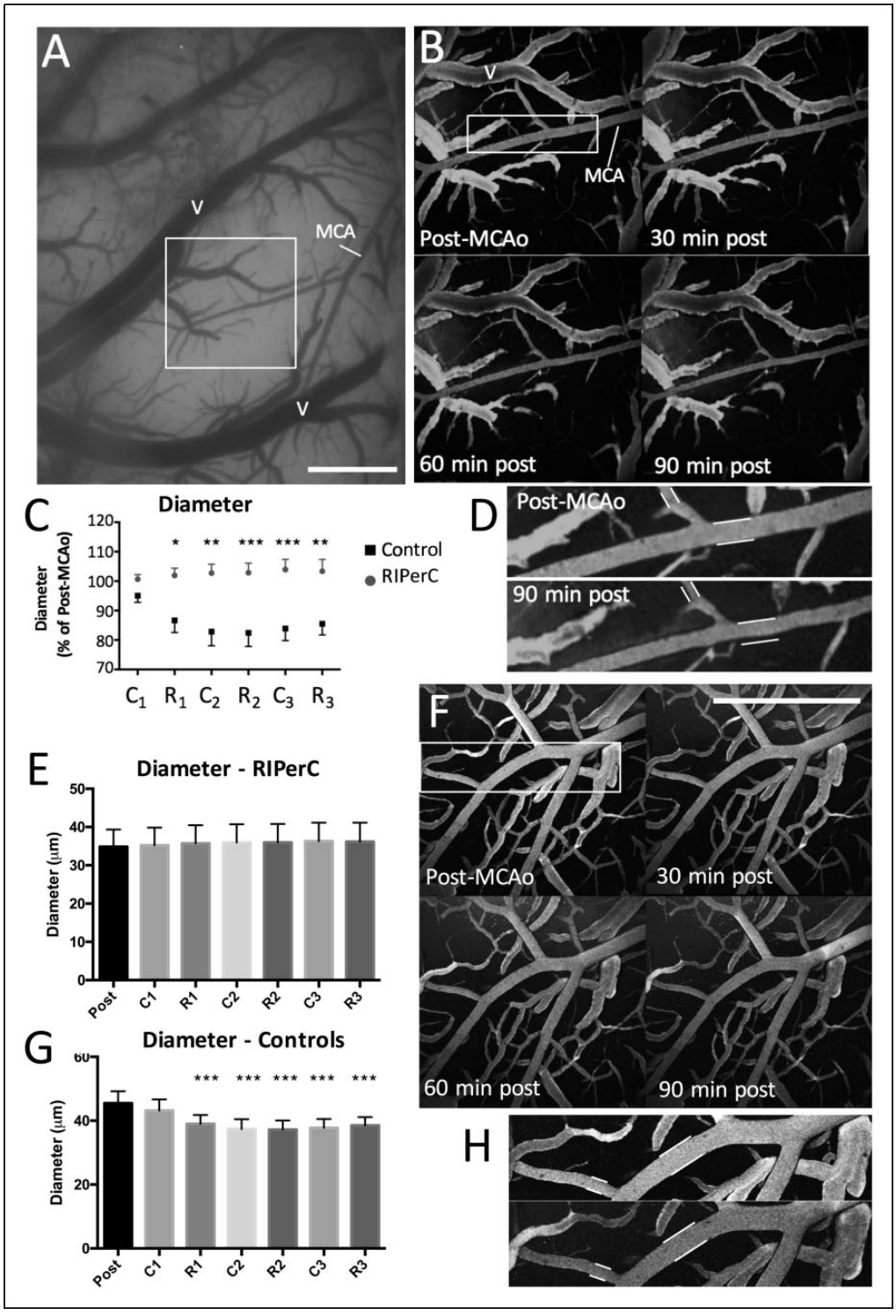

Figure 4. (a) Cranial window for two photon laser scanning microscopy (TPLSM) performed in a control rat. Scale bar, 0.5 mm. (b) Shows maximum intensity projections acquired during TPLSM of pial vessels from the region demarcated (white box) in (a). Narrowing of pial collaterals and distal MCA segments over time after MCA occlusion (MCAo) was apparent in controls ($n = 8$) (b, d) but did not occur in RIPerC-treated animals ($n = 8$) (f, h). Scale bar in F, 0.5 mm. (c) Mean arteriole diameter over time after MCAo. Sidak's post hoc comparisons revealed that RIPerC-treated rats had significantly larger diameters at all-time points after the initial BFO clamp. (e, g) Repeated measures analyses confirmed that a significant reduction in arteriole diameter occurred in control rats (g) but not in RIPerC rats (e). Post hoc comparisons confirmed significant narrowing of vessels at R1, C2, R2, C3, and R3 ($P < .001$). Graphs show mean ± s.e.m. $^{*}P < 0.05$; $^{**}P < 0.01$; $^{***}P < 0.001$. MCA: middle cerebral artery; V: surface vein; C1: 1st cycle of clamp; R1: 1st cycle of release; C2: 2nd cycle of clamp; R2: 2nd cycle of release; C3: 3rd cycle of clamp; R3: 3rd cycle of release.

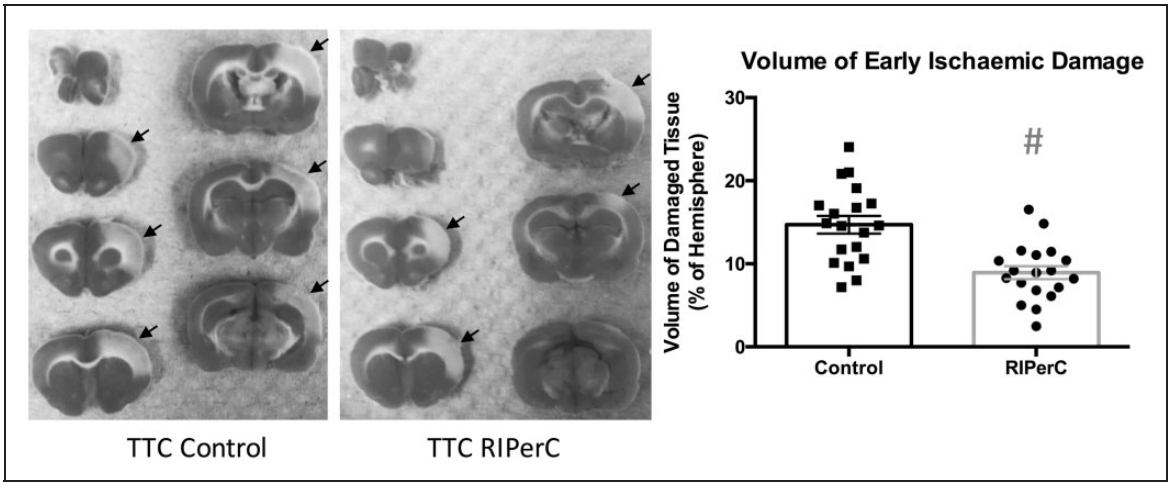

Figure 5. Infarct volume at 6-h post-MCAo (percentage of hemisphere). A significant reduction in infarct volume was observed in RIPerC-treated animals ($n = 19$) compared to controls ($n = 19$) $^{\#}P = 0.0001$. TTC, 2,3,5-triphenyltetrazolium chloride staining.

Discussion

Using LSCI and TPLSM in rats with a distal MCAo, our data demonstrate that RIPerC induces a significant increase in blood flow through pial collaterals. Notably, this increase is due to continued dilation (from post-MCAo, pre-treatment values) of pial collaterals and MCA segments adjacent or downstream to ACA-MCA connections in treated animals, contrasting with progressive constriction of these same vessels in control rats. This prevention of "collateral collapse" was associated with a significant reduction in early ischemic damage 6 h after stroke.

Cerebral blood flow and neuroprotection after RIPerC

Previous preclinical studies in mice suggest that RIPerC can improve regional cerebral blood flow after embolic MCAo.[18,20] The major finding of this study is that RIPerC improves blood flow through collateral vasculature by preventing the narrowing of these vessels over time after ischemic onset (as observed in control rats). This maintenance of post-stroke vasodilation in treated rats and narrowing of MCA segments over time in untreated rats was also observed in previous preclinical studies of transient aortic occlusion as a collateral therapeutic.[1] As transient aortic occlusion also involves ligation of a femoral artery (to allow advancement of the dilation catheter to the descending aorta) and thus results in ischemia peripheral to the brain, this raises the interesting possibility that the vasodilation induced by transient aortic occlusion may share common humoral mediators with RIPerC. Notably, transient aortic occlusion had both dilatatory effects but also induced a significant increase in blood pressure in the carotid artery that manifests as significantly increased blood flow velocity. Here, RIPerC maintained or augmented pial arteriole diameter but was not associated with increased flow velocity or an increase in systemic blood pressure, suggesting that these two mechanisms of enhanced flow after aortic occlusion may have different origins (with vasodilation resulting from humoural factors released by peripheral ischemia and increased flow velocity due to blood flow diversion from the periphery to the head that increases blood pressure above the aortic occlusion and therefore increases cerebral perfusion pressure). Neuroprotection due to transient aortic occlusion reduces infarct by ~43% (24 h after ischemic onset),[50] comparable to our reduction in early ischemic damage using 3 cycles of RIPerC (~39% reduction at 6 h post). As such, increases in flow due to diameter changes alone may be sufficient to protect vulnerable tissue (without large increases in perfusion pressure).

In preclinical studies, RIPerC improves the efficacy of neuroprotection with minocycline, recanalization with tPA, and has been associated with a reduction of infarct and neurological deficits 24 and 48 h after stroke.[13,17–21,51] Moreover, RIPerC may reduce autophagy and protect the blood–brain barrier (reducing extravasation and hemorrhagic transformation).[22] While several randomized clinical have shown RIPerC reduces myocardial infarct size in patients, clinical data in cerebral ischemia are limited.[52,53] In a recent randomized trial, investigators studied the effect of RIPerC as adjunctive therapy to intravenous rt-PA for acute ischemic stroke and assessed the feasibility of RIPerC performed during transport to hospital. The approach was found feasible, and 247 acute stroke patients received RIPerC as an adjuvant to rt-PA (196 patients received standard treatment).[23]

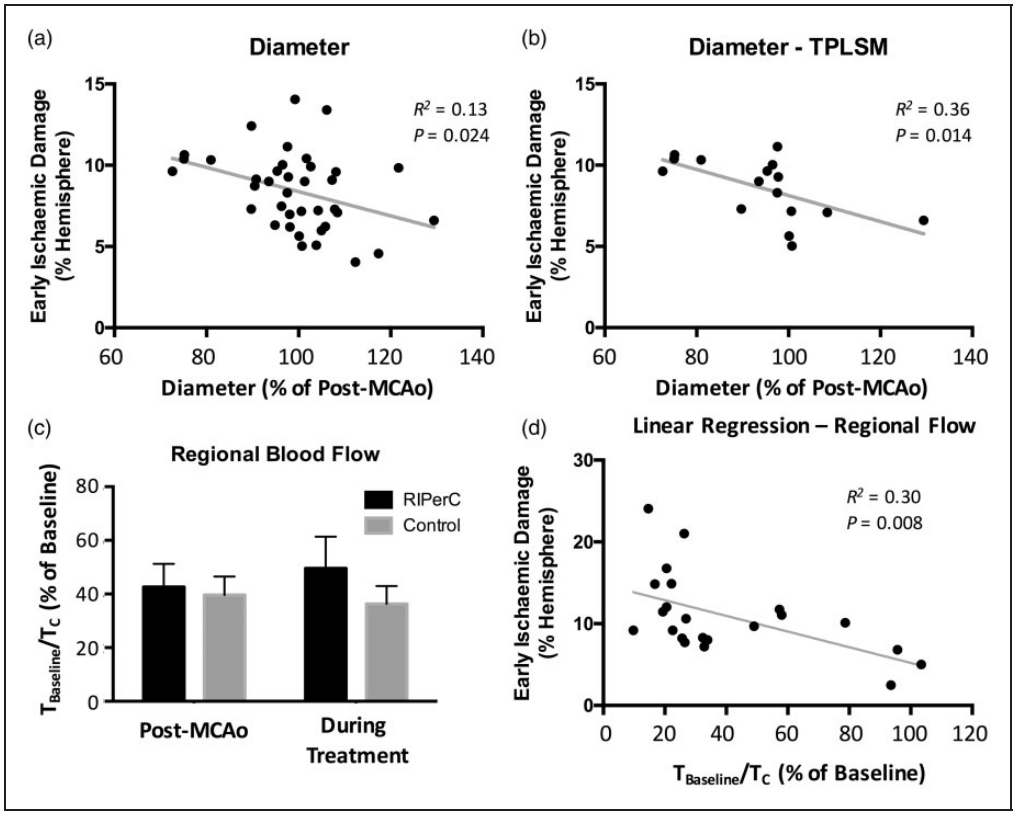

Figure 6. (a) The relationship between the diameter of the distal middle cerebral artery segments during the final imaging session (90 min after RIPerC or sham treatment onset) relative to the measurement at 60 min after middle cerebral artery occlusion (MCAo). When volume of tissue damage was examined as a function of arteriole diameter (relative to post-MCAo, collapsing all animals ($n = 38$) from both experimental groups in both laser speckle contrast imaging (LSCI) and two photon laser scanning microscopy (TPLSM) experiments into a single plot), a significant linear relationship was observed, and animals in which arterioles showed greater narrowing relative to post-MCAo measures tended to have larger volumes of ischemic damage. (b) The linear relationship was strengthened when only data from TPLSM experiments were included in the regression analysis. (c, d) The relationship between regional blood flow within the cranial window and the volume of early ischemic damage. (c) Blood flow in the region of interest in the penumbral region of the MCAo was reduced to 40% of pre-MCAo baseline prior to treatment (60 min after MCAo onset). Bars to the right of post-MCAo measures show the mean blood flow measures in the region of interest during the treatment period (i.e. the average of the $\tau_{Baseline}/\tau_C$ values derived from the six time points during RIPerC or sham treatment). There was no main effect of RIPerC on regional flow ($P > .05$). (d) However, regional flow was predictive of ischemic damage, as a linear relationship between regional flow and volume of early tissue damage (again collapsing all animals from LSCI and TPLSM studies onto a single plot) was observed, with volume of damage increasing with reducing regional flow.

Although the study reported neutral results on follow-up measures, a tissue survival analysis suggested that prehospital RIPerC was neuroprotective.

Our data also suggest that RIPerC significantly reduces early ischemic damage. Notably, tissue damage was significantly dependent on the diameter of the pial arterioles, as increased narrowing of the pial arterioles (from post-MCAo measures) was associated with increased volume of ischemic damage (Figure 6(a) and (b)). However, it is important to note that these diameter measures are relative to values post-MCAo but prior to treatment (i.e. at a time point when arterioles are likely dilated relative to pre-stroke baseline), and we do not have measures of how dilated each vessel was relative to baseline. Consequently, an even stronger statistical relationship may be determined by studies that measure narrowing relative pre-stroke values. Interestingly, while RIPerC did not have a significant effect on blood flow velocity in LSCI or TPLSM studies (whether measuring within arterioles or using a regional measure), early ischemic damage did vary as a function of regional blood flow (Figure 6(d)). Given that regional measures of speckle contrast are highly correlated with other measures of regional cerebral blood flow such as laser Doppler flowmetry[49] that reflect overall tissue flow and have previously been shown to be predictive of degree of ischemia, this relationship is not surprising. Combined, our data show that overall blood flow predicts tissue fate and identify prevention of cerebral arteriole narrowing as a protective effect of RIPerC treatment.

This neuroprotective effect likely results from both increases in blood flow that shift penumbral flow beyond critical values for tissue viability, from maintenance of the integrity of the blood–brain barrier in ischemic regions, and from the release of humoral factors at the site of peripheral ischemia that confer neuroprotection in the brain.[13,22]

Summary and next steps

Our data define collateral flow augmentation via prevention of collateral collapse as an important neuroprotective mechanism during RIPerC. Further preclinical and clinical study is required to allow for optimal clinical translation. While the prevention of collateral collapse by RIPerC was consistent across two anesthetics used in this study (isoflurane and urethane), the exact relationship between collateral flow and infarct progression would be most accurately described in awake, non-anaesthetized animals. Additionally, while most preclinical studies of RIPerC are performed on rodent hind limbs via femoral ligation,[13,17–22,54] clinical studies generally involve upper limb ischemia via inflation blood pressure cuff.[16,23] Differences in the hemodynamic and neuroprotective effects of different paradigms of remote ischemia need to be systematically assessed. Moreover, the time of application of RIPerC, the number of RIPerC cycles, and the ischemic duration in each cycle of RIPerC vary between different published papers.[13,17–22,54] Defining the optimal parameters for RIPerC would be aided by identification of humoral factors associated with its hemodynamic or neuroprotective effects. Identification of the molecular mechanisms of RIPerC would allow pharmacotherapy with drugs which share common effectors.[55]

Funding

The author(s) disclosed receipt of the following financial support for the research, authorship, and/or publication of this article: Research supported by the Heart and Stroke Foundation of Canada (IRW, AS), the Canadian Institutes of Health Research (IRW), and Alberta Innovates Health Solutions (IRW). JM was supported by the Li Ka Shing Sino-Canadian Exchange Program. MVB received support from the Neuroscience and Mental Health Institute and a Queen Elizabeth II Graduate Scholarship.

Declaration of conflicting interests

The author(s) declared no potential conflicts of interest with respect to the research, authorship, and/or publication of this article.

Authors' contributions

JM, YM, and BD performed surgeries and imaging experiments. MVB performed two-photon imaging (with JM) and image analysis (with JM and IRW). AS and IW designed the experiments, and JM and IRW made final figures and wrote the manuscript.

References

1. Winship IR, Armitage GA, Ramakrishnan G, et al. Augmenting collateral blood flow during ischemic stroke via transient aortic occlusion. *J Cereb Blood Flow Metab* 2014; 34: 61–71.
2. Liebeskind DS. Collateral circulation. *Stroke* 2003; 34: 2279–2284.
3. Shuaib A, Butcher K, Mohammad AA, et al. Collateral blood vessels in acute ischaemic stroke: a potential therapeutic target. *Lancet Neurol* 2011; 10: 909–921.
4. Ramakrishnan GAG and Winship IR. Understanding and augmenting collateral blood flow during ischemic stroke. In: Julio CGR (ed.) *Acute ischemic stroke*. Rijeka, Croatia: InTech, 2012.
5. Hendrikse J, van Raamt AF, van der Graaf Y, et al. Distribution of cerebral blood flow in the circle of Willis. *Radiology* 2005; 235: 184–189.
6. Winship IR. Cerebral collaterals and collateral therapeutics for acute ischemic stroke. *Microcirculation* 2015; 22: 228–236.
7. Bang OY, Saver JL, Buck BH, et al. Impact of collateral flow on tissue fate in acute ischaemic stroke. *J Neurol Neurosurg Psychiatr* 2008; 79: 625–629.
8. Bang OY, Saver JL, Kim SJ, et al. Collateral flow predicts response to endovascular therapy for acute ischemic stroke. *Stroke* 2011; 42: 693–699.
9. Christoforidis GA, Mohammad Y, Kehagias D, et al. Angiographic assessment of pial collaterals as a prognostic indicator following intra-arterial thrombolysis for acute ischemic stroke. *Am J Neuroradiol* 2005; 26: 1789–1797.
10. Schellinger PD, Kohrmann M, Liu S, et al. Favorable vascular profile is an independent predictor of outcome: a post hoc analysis of the safety and efficacy of NeuroFlo Technology in Ischemic Stroke trial. *Stroke* 2013; 44: 1606–1608.
11. Liebeskind DS. Of mice and men: essential considerations in the translation of collateral therapeutics. *Stroke* 2008; 39: e187–e188; author reply e9.
12. Murry CE, Jennings RB and Reimer KA. Preconditioning with ischemia: a delay of lethal cell injury in ischemic myocardium. *Circulation* 1986; 74: 1124–1136.
13. Hess DC, Hoda MN and Bhatia K. Remote limb perconditioning [corrected] and postconditioning: will it translate into a promising treatment for acute stroke? *Stroke* 2013; 44: 1191–1197.
14. Lim SY and Hausenloy DJ. Remote ischemic conditioning: from bench to bedside. *Front Physiol* 2012; 3: 27.
15. Wang Y, Reis C, Applegate R, et al. Ischemic conditioning-induced endogenous brain protection: applications pre-, per- or post-stroke. *Exp Neurol* 2015; 272: 26–40.
16. Hougaard KD, Hjort N, Zeidler D, et al. Remote ischemic perconditioning in thrombolysed stroke patients:

randomized study of activating endogenous neuroprotection – design and MRI measurements. *Int J Stroke* 2013; 8: 141–146.
17. Hahn CD, Manlhiot C, Schmidt MR, et al. Remote ischemic per-conditioning: a novel therapy for acute stroke? *Stroke* 2011; 42: 2960–2962.
18. Hoda MN, Siddiqui S, Herberg S, et al. Remote ischemic perconditioning is effective alone and in combination with intravenous tissue-type plasminogen activator in murine model of embolic stroke. *Stroke* 2012; 43: 2794–2799.
19. Hoda MN, Fagan SC, Khan MB, et al. A 2 x 2 factorial design for the combination therapy of minocycline and remote ischemic perconditioning: efficacy in a preclinical trial in murine thromboembolic stroke model. *Exp Transl Stroke Med* 2014; 6: 10.
20. Hoda MN, Bhatia K, Hafez SS, et al. Remote ischemic perconditioning is effective after embolic stroke in ovariectomized female mice. *Transl Stroke Res* 2014; 5: 484–490.
21. Baskar Jesudasan SJ, Todd KG and Winship IR. Reduced inflammatory phenotype in microglia derived from neonatal rat spinal cord versus brain. *PloS One* 2014; 9: e99443.
22. Ren C, Li N, Wang B, et al. Limb ischemic perconditioning attenuates blood-brain barrier disruption by inhibiting activity of MMP-9 and occludin degradation after focal cerebral ischemia. *Aging Dis* 2015; 6: 406–417.
23. Hougaard KD, Hjort N, Zeidler D, et al. Remote ischemic perconditioning as an adjunct therapy to thrombolysis in patients with acute ischemic stroke: a randomized trial. *Stroke* 2014; 45: 159–167.
24. Hanss M. Letter by Hanss regarding article, ''Remote ischemic perconditioning is effective alone and in combination with intravenous tissue-type plasminogen activator in murine model of embolic stroke''. *Stroke* 2013; 44: e36.
25. Kim T, Masamoto K, Fukuda M, et al. Frequency-dependent neural activity, CBF, and BOLD fMRI to somatosensory stimuli in isoflurane-anesthetized rats. *Neuroimage* 2010; 52: 224–233.
26. Masamoto K, Fukuda M, Vazquez A, et al. Dose-dependent effect of isoflurane on neurovascular coupling in rat cerebral cortex. *Eur J Neurosci* 2009; 30: 242–250.
27. Masamoto K, Kim T, Fukuda M, et al. Relationship between neural, vascular, and BOLD signals in isoflurane-anesthetized rat somatosensory cortex. *Cereb Cortex* 2007; 17: 942–950.
28. Santisakultarm TP, Kersbergen CJ, Bandy DK, et al. Two-photon imaging of cerebral hemodynamics and neural activity in awake and anesthetized marmosets. *J Neurosci Meth* 2016; 271: 55–64.
29. Seto A, Taylor S, Trudeau D, et al. Induction of ischemic stroke in awake freely moving mice reveals that isoflurane anesthesia can mask the benefits of a neuroprotection therapy. *Front Neuroenerget* 2014; 6: 1.
30. Lay CC and Frostig RD. Complete protection from impending stroke following permanent middle cerebral artery occlusion in awake, behaving rats. *Eur J Neurosci* 2014; 40: 3413–3421.
31. Lay CC, Jacobs N, Hancock AM, et al. Early stimulation treatment provides complete sensory-induced protection from ischemic stroke under isoflurane anesthesia. *Eur J Neurosci* 2013; 38: 2445–2452.
32. Ramakrishnan G, Dong B, Todd KG, et al. Transient aortic occlusion augments collateral blood flow and reduces mortality during severe ischemia due to proximal middle cerebral artery occlusion. *Transl Stroke Res* 2016; 7: 149–155.
33. Hara K and Harris RA. The anesthetic mechanism of urethane: the effects on neurotransmitter-gated ion channels. *Anesth Analg* 2002; 94: 313–318.
34. Maggi CA and Meli A. Suitability of urethane anesthesia for physiopharmacological investigations in various systems. Part 2: cardiovascular system. *Experientia* 1986; 42: 292–297.
35. Maggi CA and Meli A. Suitability of urethane anesthesia for physiopharmacological investigations in various systems. Part 1: general considerations. *Experientia* 1986; 42: 109–114.
36. Paasonen J, Salo RA, Shatillo A, et al. Comparison of seven different anesthesia protocols for nicotine pharmacologic magnetic resonance imaging in rat. *Eur Neuropsychopharmacol* 2016; 26: 518–531.
37. Winship IR. Laser speckle contrast imaging to measure changes in cerebral blood flow. *Meth Mol Biol* 2014; 1135: 223–235.
38. Armitage GA, Todd KG, Shuaib A and Winship IR. Laser speckle contrast imaging of collateral blood flow during acute ischemic stroke. *J Cereb Blood Flow Metab* 2010; 30: 1432–1436.
39. Li N, Thakor NV and Jia X. Laser speckle imaging reveals multiple aspects of cerebral vascular responses to whole body mild hypothermia in rats. *Conf Proc IEEE Eng Med Biol Soc* 2011; 2011: 2049–2052.
40. Boas DA and Dunn AK. Laser speckle contrast imaging in biomedical optics. *J Biomed Opt* 2010; 15: 011109.
41. Dunn AK. Laser speckle contrast imaging of cerebral blood flow. *Ann Biomed Eng* 2012; 40: 367–377.
42. Strong AJ, Bezzina EL, Anderson PJ, et al. Evaluation of laser speckle flowmetry for imaging cortical perfusion in experimental stroke studies: quantitation of perfusion and detection of peri-infarct depolarisations. *J Cereb Blood Flow Metab* 2006; 26: 645–653.
43. Fischer MJ, Uchida S and Messlinger K. Measurement of meningeal blood vessel diameter in vivo with a plug-in for ImageJ. *Microvasc Res* 2010; 80: 258–266.
44. Tennant KA and Brown CE. Diabetes augments in vivo microvascular blood flow dynamics after stroke. *J Neurosci* 2013; 33: 19194–19204.
45. Shih AY, Driscoll JD, Drew PJ, et al. Two-photon microscopy as a tool to study blood flow and neurovascular coupling in the rodent brain. *J Cereb Blood Flow Metab* 2012; 32: 1277–1309.
46. Chen ST, Hsu CY, Hogan EL, et al. A model of focal ischemic stroke in the rat: reproducible extensive cortical infarction. *Stroke* 1986; 17: 738–743.
47. Swanson RA, Morton MT, Tsao-Wu G, et al. A semiautomated method for measuring brain infarct volume. *J Cereb Blood Flow Metab* 1990; 10: 290–293.

48. Lin TN, He YY, Wu G, et al. Effect of brain edema on infarct volume in a focal cerebral ischemia model in rats. *Stroke* 1993; 24: 117–121.
49. Ayata C, Dunn AK, Gursoy-Ozdemir Y, et al. Laser speckle flowmetry for the study of cerebrovascular physiology in normal and ischemic mouse cortex. *J Cereb Blood Flow Metab* 2004; 24: 744–755.
50. Noor R, Wang CX, Todd K, et al. Partial intra-aortic occlusion improves perfusion deficits and infarct size following focal cerebral ischemia. *J Neuroimaging* 2010; 20: 272–276.
51. Ren C, Gao M, Dornbos D 3rd, et al. Remote ischemic post-conditioning reduced brain damage in experimental ischemia/reperfusion injury. *Neurol Res* 2011; 33: 514–519.
52. Botker HE, Kharbanda R, Schmidt MR, et al. Remote ischaemic conditioning before hospital admission, as a complement to angioplasty, and effect on myocardial salvage in patients with acute myocardial infarction: a randomised trial. *Lancet* 2010; 375: 727–734.
53. White SK, Frohlich GM, Sado DM, et al. Remote ischemic conditioning reduces myocardial infarct size and edema in patients with ST-segment elevation myocardial infarction. *JACC Cardiovasc Interv* 2015; 8: 178–188.
54. Pan J, Li X and Peng Y. Remote ischemic conditioning for acute ischemic stroke: dawn in the darkness. *Rev Neurosci* 2016.
55. Zhao H, Ren C, Chen X, et al. From rapid to delayed and remote postconditioning: the evolving concept of ischemic postconditioning in brain ischemia. *Curr Drug Targets* 2012; 13: 173–187.